Towards an optimized all lattice-matched InAlAs/InGaAsP/InGaAs multijunction solar cell with efficiency >50%

Marina S. Leite,[1,2,3,a)] Robyn L. Woo,[4] Jeremy N. Munday,[1,5] William D. Hong,[4] Shoghig Mesropian,[4] Daniel C. Law,[4] and Harry A. Atwater[1]
[1]*J. Thomas Watson Department of Applied Physics, California Institute of Technology, 1200 E California Blvd., Pasadena, California 91125-9500, USA*
[2]*Center for Nanoscale Science and Technology, National Institute of Standards and Technology, Gaithersburg, Maryland, USA*
[3]*Maryland NanoCenter, University of Maryland, College Park, Maryland, USA*
[4]*Boeing-Spectrolab Inc., 12500 Gladstone Avenue, Sylmar, California 91342, USA*
[5]*Department of Electrical and Computer Engineering and The Institute for Research in Electronics and Applied Physics, University of Maryland, College Park, Maryland 20742, USA*

(Received 14 September 2012; accepted 26 September 2012; published online 22 January 2013)

An approach for an all lattice-matched multijunction solar cell optimized design is presented with 5.807 Å lattice constant, together with a detailed analysis of its performance by means of full device modeling. The simulations show that a (1.93 eV)$In_{0.37}Al_{0.63}As$/(1.39 eV)$In_{0.38}Ga_{0.62}As_{0.57}P_{0.43}$/(0.94 eV)$In_{0.38}Ga_{0.62}As$ 3-junction solar cell can achieve efficiencies >51% under 100-suns illumination (with $V_{oc} = 3.34$ V). As a key proof of concept, an equivalent 3-junction solar cell lattice-matched to InP was fabricated and tested. The independently connected single junction solar cells were also tested in a spectrum splitting configuration, showing similar performance to a monolithic tandem device, with $V_{oc} = 1.8$ V. © *2013 American Institute of Physics*. [http://dx.doi.org/10.1063/1.4758300]

Multijunction solar cells (MJSCs) are one of the most promising options to efficiently convert the sunlight into electricity. In a multijunction device, each subcell absorbs and converts the sunlight from a specific region of the sun spectrum. Because the photon power conversion efficiency is maximum when the band gap energy (E_g) of a material is equal to the incident photon energy ($h\nu$), each subcell is designed to have a specific band gap in order to maximize the power conversion over the whole solar spectrum.[1–4] There are essentially two ways of splitting the spectrum in MJSCs. The first one is by using beam-splitting filters to efficiently distribute the light between all subcells, which allows for the use of independent single junction cells in a parallel, series, or another specific architecture.[5] The second, a currently common approach, is to arrange the subcells in a mechanically stacked configuration or a tandem system, where the sunlight strikes the highest band gap subcell first, and progressively hits the lower band gap subcells. The advantage of this configuration is the fact that each subcell absorbs any light with energy higher than E_g, acting as a low-pass photon energy filter. Hence, each subcell transmits only the sub-bandgap light. MJSCs are currently successfully employed in concentrator photovoltaic (CPV) technologies, in which lenses and mirrors focus the sunlight on a small area solar cell, significantly decreasing the amount of material required and, consequently, the overall cost of the photovoltaic device. In this arrangement, ultra-high efficiencies can be achieved by using high-quality material and the appropriate combination of band gaps.[6] Generally, compound semiconductors are used for fabricating MJSCs because these alloys have band gaps ranging from 0.3 to 2.3 eV, covering most of the solar spectrum. Nevertheless, there is an urgent search for a monolithic design that will convert sunlight into electricity with practical efficiencies (η) higher than 50%.[7]

GaAs and Ge lattice-matched semiconductor compounds were originally used to fabricate dual junction solar cells.[8,9] With the addition of an active Ge subcell, upright 3-junction solar cells with both lattice-matched and metamorphic InGaP/(In)GaAs/Ge designs have achieved over 40% efficiency.[10,11] These designs have achieved 41.6% efficiency under 364 suns for lattice-matched cells,[12] as well as 41.6% efficiency at 484 suns for upright metamorphic 3-junction cells,[13] and can achieve more than 30% in efficiency under 1-sun global illumination, with V_{oc} equal to 2.6 V. Current-matching for such cells is a major constraint for further improvement of efficiencies. One way around this limitation is an inverted metamorphic multijunction (IMM) design, which enables better band gap energy combinations. Recently, an IMM approach achieved 43.5% under concentrated sunlight by using a combination of InGaP/GaAs/InGaAs subcells. However, further improvements will likely be limited by threading dislocations because of the lattice-mismatch. Dilute nitrides formed by $In_xGa_{1-x}As_yN_{1-y}$ have also been successfully implemented in 3-junction solar cells lattice-matched to GaAs, which have independently tunable band gaps and lattice constants.[14] To date, the world record 3-junction solar cell (43.5% under 418-suns illumination) utilizes this alloy as the middle 1 eV subcell, allowing for a better current match between the different subcells. One promising combination of III-V direct band gap semiconductor materials is based on InP lattice constant.[15,16] To date, a three-terminal InP/InGaAs dual junction cell showed 31.8% efficiency under 50-suns, a promising option for CPV.[17]

a)Author to whom correspondence should be addressed. Electronic mail: marina.leite@nist.gov.

Here, we report on an optimized band gap combination for a monolithic 3-junction III-V semiconductor solar cell, formed by (1.93 eV) $In_{0.37}Al_{0.63}As$/(1.39 eV) $In_{0.38}Ga_{0.62}$ $As_{0.57}P_{0.43}$/(0.94 eV) $In_{0.38}Ga_{0.62}As$ with lattice constant equal to 5.807 Å. We compare the theoretical performance of the proposed device with the conventional GaAs-based design and to an alternative InP-based design. According to full device simulations, this proposed approach for MJSCs can achieve theoretical efficiencies >51% under merely 100-suns illumination. As a key proof of concept on the band gap and material combination, we have fabricated each independent subcell lattice-matched to InP–(1.47 eV) $In_{0.52}Al_{0.48}As$/(1.06 eV) $In_{0.53}Ga_{0.47}As_{0.42}P_{0.58}$/(0.74 eV) $In_{0.53}Ga_{0.47}As$. The maximum external quantum efficiency (EQE) of each subcell is around 80%. A monolithic 3J was fabricated and tested under direct illumination and showed an open circuit voltage (V_{oc}) equal to 1.8 V, demonstrating the tandem activity of the device and the high performance of the tunnel junctions. The results presented here indicate that the monolithic 3-junction solar cells can be implemented as an alternative for ultra-high efficiency MJSCs.

Figure 1(a) shows the band gap energy diagram as a function of lattice constant for various III-V compound semiconductor materials. Historically, alloys lattice-matched to GaAs/Ge (blue dashed line) were originally used to fabricate high efficiency multijunction solar cells.[10,11] In particular, the (1.90 eV) InGaP/(1.42 eV) GaAs/(0.67 eV) Ge combination—represented by blue solid squares—has received considerable attention in the past decades, due to the well-known optical properties of the alloys, as well as the capability of growing high crystalline InGaP on GaAs. However, the poor current-matching between the subcells (total current density J_{tot} in tandem configuration is equal to 20.5, 10.4, and 29.8 mA/cm^2, from top to bottom, for the terrestrial spectrum) limits the overall performance of the device.

In order to identify the best III-V direct band gap semiconductor materials combination for a monolithic *all* lattice-matched 3-junction solar cell, detailed balance calculations were performed for all possible band gap arrangements with lattice spacing between GaAs (5.653 Å) and InP (5.868 Å), using AM1.5 direct illumination. The detailed balance model used here assumes: 300 K for all calculations, no reflection losses, no series-resistance losses, no reabsorption of emitted photons between different subcells, transparent zero-resistance tunnel junction interconnects, an enforced current-match between the subcells [V_{3J} (I) = ΣV_i (I)], and the illumination of a blackbody into a hemisphere. Figure 1(b) displays the theoretical efficiency as a function of sunlight concentration for four series-connected distinct designs: (i) GaAs lattice-matched existing 3-junction cells (blue squares), (ii) the IMM approach (blue circles), (iii) InP lattice-matched alloys (green diamonds), and (iv) an optimized 3-junction (red triangles) formed by a combination of (1.93 eV) $In_{0.37}Al_{0.63}As$/(1.39 eV) $In_{0.38}Ga_{0.62}As_{0.57}P_{0.43}$/(0.94 eV) $In_{0.38}Ga_{0.62}$ As alloys. The optimized 3-junction[18] can achieve ideal efficiencies higher than 50% under just 30-suns illumination. The best IMM design performs better than the equivalent lattice-matched one; nevertheless, the proposed all lattice-matched optimized design surpasses its performance.

Currently, MJSCs have achieved 80%–90% of their theoretical efficiencies; therefore, it is crucial to analyze the

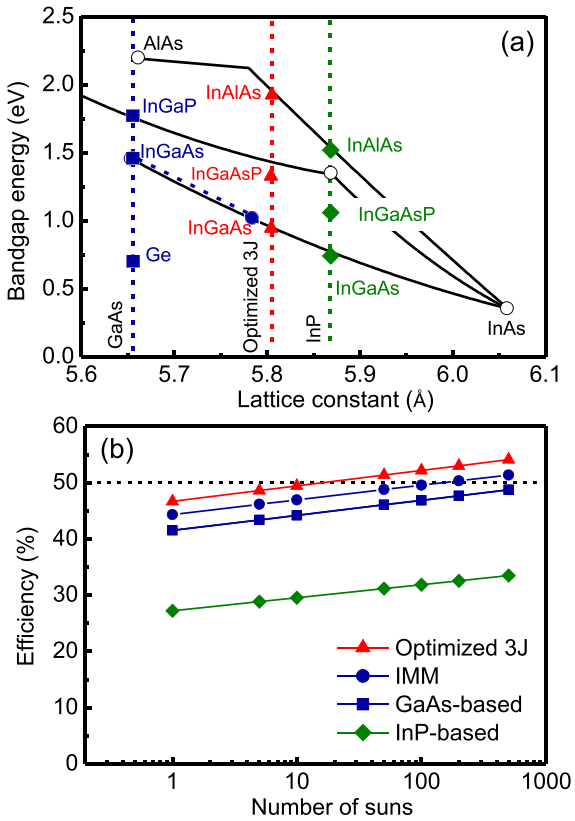

FIG. 1. (a) Energy band gap diagram as a function of lattice spacing for selected III-V compound semiconductor materials. The substrates' lattice spacings are represented by open circles. The alloys of the 3-junction lattice-matched existing Ge and GaAs-based designs are indicated by blue squares, and the IMM 1.8 eV InGaP/1.4 eV GaAs/1.0 eV InGaAs approach by blue circles. The proposed lattice-matched design, formed by (1.93 eV) $In_{0.37}Al_{0.63}As$/(1.39 eV) $In_{0.38}Ga_{0.62}As_{0.57}P_{0.43}$/(0.94 eV) $In_{0.38}Ga_{0.62}As$, with optimized band gaps and lattice spacing = 5.807 Å, is displayed as red triangles. The green diamonds correspond to an InP-based approach, which involves the same alloyed semiconductors as the optimized 3-junction: (1.47 eV) $In_{0.52}Al_{0.48}As$/(1.06 eV) $In_{0.53}Ga_{0.47}As_{0.42}P_{0.58}$/(0.74 eV) $In_{0.53}Ga_{0.47}As$. (b) Efficiency as a function of number of suns (light intensity) obtained by detailed balance calculation for the four different triple-junction designs shown in (a), in a two-terminal series-connection configuration. All calculations were performed assuming constant temperature (300 K). Note that the optimized 3-junction design (red triangles) can ideally achieve more than 50% in efficiency under merely 30-suns illumination.

performance of these devices under ideal conditions. Thus, the suggested tandem design could, in principle, achieve $\eta > 48\%$ under 500-suns illumination. The efficiency of the 3-junction cell enhances logarithmically with light intensity (i.e., number of suns) until 1000-suns illumination, as a consequence of the photovoltage increase. Furthermore, one can expect efficiencies >50% at high injection levels.

For a realistic estimation of the performance of an achievable lattice-matched 3J design, 1-dimensional full device simulations were performed for the optimized band gap combination. The modeling[19] was performed assuming Lambert-Beer absorption (no reflection losses), normal incidence of light, a *p*-type base and a *n*-type emitter for all subcells, abrupt *p-n* junctions, constant temperature (300 K), direct 1-sun (90 mW/cm^2), and concentrated illumination. For every layer used in the device modeling, we considered material composition, lattice constant, thickness, dielectric constant, electron affinity, band gap, effective conduction and valence band densities, electron and hole motilities, the

TABLE I. Materials, band gaps and thicknesses of each subcell forming the (1.93 eV) InAlAs/(1.39 eV) InGaAsP/(0.94 eV) InGaAs monolithic lattice-matched 3-junction suggested device with optimized band gap combination. The tunnel junctions are omitted since the simulations assumed zero-loss resistance junctions.

	Layer	Alloy	Eg (eV)	Thickness (μm)
Top subcell	Window	$In_{0.30}Al_{0.70}As$	2.10	0.02
	Emitter	$In_{0.37}Al_{0.63}As$	1.93	0.20
	Base	$In_{0.37}Al_{0.63}As$	1.93	2.00
	Back surface field	$In_{0.30}Al_{0.70}As$	2.10	0.02
Middle subcell	Window	$In_{0.37}Al_{0.63}As$	1.93	0.02
	Emitter	$In_{0.38}Ga_{0.62}As_{0.57}P_{0.43}$	1.39	0.20
	Base	$In_{0.38}Ga_{0.62}As_{0.57}P_{0.43}$	1.39	2.00
	Back surface field	$In_{0.37}Al_{0.63}As$	1.93	0.02
Bottom subcell	Window	$In_{0.85}Ga_{0.15}P$	1.43	0.02
	Emitter	$In_{0.38}Ga_{0.62}As$	0.94	0.20
	Base	$In_{0.38}Ga_{0.62}As$	0.94	2.00
	Back surface field	$In_{0.85}Ga_{0.15}P$	1.43	0.02

doping concentration of shallow acceptors and donors, the thermal velocity of electrons and holes, the alloy density, Auger recombination for electrons and holes, and direct band-to-band recombination. Additionally, we also took into account how many photons with a specific wavelength are absorbed and reflected by each layer based on its dielectric properties (n,k), which were used to calculate the corresponding spectral absorption coefficient. These values were calculated based on an ellipsometer database and by using Vegard's law for the layers at 5.807 Å. For the multijunction device modeling, we assumed transparent and zero-resistance tunnel junction interconnects, and again enforced current-matching between individually modeled subcells.

Table I displays the composition, band gap energy, and thickness of each layer used in the simulations presented. *P*-type bases and *n*-type emitters form the mechanical stack. In all cases, window and back surface field layers were used to reduce surface recombination and the scattering of carriers towards the tunnel junction, respectively. These layers were carefully chosen to be transparent to wavelengths absorbed by the subsequent lower band gap *p*-*n* layer. The successful fabrication of the 1.93 eV InAlAs top subcell requires the growth of alloys with high Al content (0.63 in fraction for the *p*-*n* absorber layer and 0.70 in fraction for the 2.10 eV window and back surface field layers) with a tensile strain of +0.47%. We have previously demonstrated the growth of dislocation-free epitaxial $In_{0.35}Al_{0.65}As/In_{0.52}Al_{0.48}As$ heterostructures with strain equal to +1.17%[20] (2.5 times larger than what is required for the optimized top subcell). Therefore, a simple extension of the same metal-organic vapor phase epitaxy (MOVPE) growth conditions should provide us high quality materials. For both the middle and bottom subcells, lattice-matched window and back surface field layers with a band gap 0.5 eV higher than that of the *p*-*n* absorber layer are available, as shown in Table I. The assumption of zero-loss tunnel junctions is reasonable due to the fact that an InP-based fabricated tandem multijunction solar cell presented the same performance as the equivalent independently connected subcells, as will be presented later.

The performance of the monolithic two-terminal (1.93 eV) $In_{0.37}Al_{0.63}As$/(1.39 eV) $In_{0.38}Ga_{0.62}As_{0.57}P_{0.43}$/(0.94 eV) $In_{0.38}Ga_{0.62}As$ series-connected optimized design [(see schematic in Figure 2(a)] was analyzed by the 1-dimensional device modeling of each individual subcell, as well as the tandem 3J solar cell. Table II summarizes the performance characteristics of all individual subcells under AM 1.5 direct illumination. The proposed approach presents a very good current-match: the total current (J_{tot}) is equal to 15.3, 18.5, and 16.8 mA/cm^2, from top to bottom. As shown

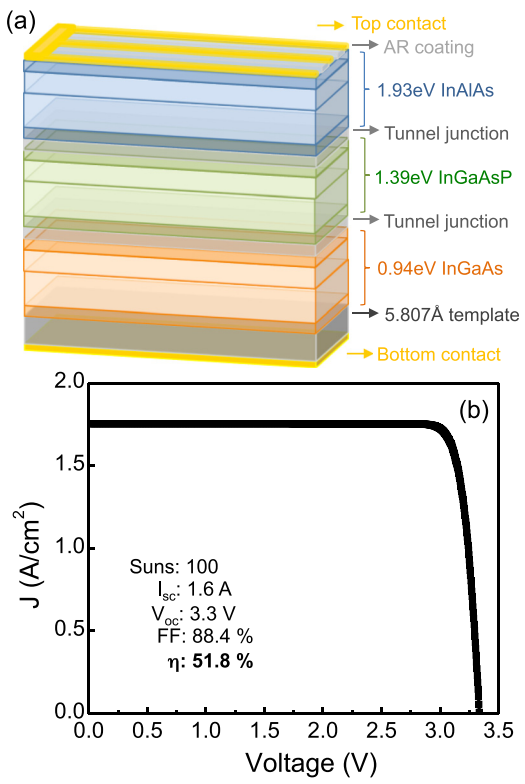

FIG. 2. (a) Schematic of a monolithic two-terminal series-connected (1.93 eV) $In_{0.37}Al_{0.63}As$/(1.39 eV) $In_{0.38}Ga_{0.62}As_{0.57}P_{0.43}$/(0.94 eV) $In_{0.38}Ga_{0.62}As$ 3-junction solar cell with an optimized band gap energies combination, and lattice constant equal to 5.807 Å, as represented by red triangles in Figure 1(a). P- and n-type layers are base and emitter, respectively. The layers are out of scale to better represent the different alloys involved in the design, and the window layers are omitted here for simplicity. (b) Light *J*-*V* curve obtained from 1-dimensional full device modeling for the 3-junction solar cell shown in (a). Note that >51% in efficiency is achieved for concentration illumination. The simulation was performed using AM 1.5 direct 100-suns illumination, assuming zero-resistance tunnel junctions.

TABLE II. Figures of merit for all individual subcells in a tandem configuration and for the optimized (1.93 eV) $In_{0.37}Al_{0.63}As$/(1.39 eV) $In_{0.38}Ga_{0.62}As_{0.57}P_{0.43}$/(0.94 eV) $In_{0.38}Ga_{0.62}As$ 3-junction device obtained from 1-dimensional device modeling, assuming Lambert-Beer absorption, normal incidence of light, constant temperature (300 K), and AM 1.5 direct 1-sun illumination.

Optimized design	V_{oc} (V)	J_{sc} (mA/cm^2)	FF (%)	η (%)
1.93 eV InAlAs	1.39	13.06	90.7	19.4
1.39 eV InGaAsP	0.98	15.78	88.0	13.7
0.94 eV InGaAs	0.64	16.50	83.6	8.9
3-junction	3.01	13.06	92.2	40.4

in Table II, the optimized lattice-matched 3-junction presents $V_{oc} = 3.01$ V and $\eta = 40.4\%$ under AM 1.5 direct illumination. This efficiency is lower than the detailed balance result (46.7%) due to the consideration of Auger and other recombination phenomena, indicating a realistic description for the device modeling. Since MJSCs are usually used in CPV systems, we also performed simulations under concentrated direct illumination. By re-optimizing the thickness of the top subcell the suggested design can achieve 51.8% efficiency under 100-suns, as shown in Figure 2(b). This result demonstrates the promising potential of our design as an achievable pathway for ultra-high efficiency solar cells.

The implementation of the suggested design requires a crystalline template with lattice constant = 5.807 Å [see red dashed line in Figure 1(a)] to initiate the epitaxial growth. The realization of such a template was achieved by the strain engineering of single crystalline layers, as recently demonstrated.[21] Although the fabrication of this MJSC involves expensive materials, its cost can be significantly decreased by performing multiple templates' growth using one bulk substrate combined with the epitaxial lift-off technique.

A first critical step for the demonstration of the optimized 3-junction solar cell is the fabrication of high-quality $In_xAl_{1-x}As$, $In_xGa_{1-x}As_yP_{1-y}$ and $In_xGa_{1-x}As$ with specific compositions. Therefore, as a proof of principle for the potential implementation of the optimized monolithic, lattice-matched, 3-junction solar cell, we fabricated and tested equivalent subcells lattice-matched to InP, which involves the same class of compound semiconductors. This alternative design—(1.47 eV) $In_{0.52}Al_{0.48}As$/(1.06 eV) $In_{0.53}Ga_{0.47}As_{0.42}P_{0.58}$/(0.74 eV) $In_{0.53}Ga_{0.47}As$—is displayed by solid green diamonds in Figure 1(a). The solar cells were grown on 50 mm, *p*-type InP (001) on-axis substrates using Veeco E400 MOVPE reactor operated at low pressure. The main precursors used in the layers are trimethylindium, trimethylaluminum, and arsine. Growth temperatures typically ranged from 600 to 750 °C depending on the layers.[22]

To test the subcells, electrical measurements were performed using a solar simulator with AM1.5 global 1-sun illumination (1 kW/m^2). One of the major limiting factors of a high efficiency MJSC is the short circuit current (J_{sc}), which will determine how much current will flow once the device is connected to a circuit. Here, all subcells were engineered to current-match at 12.0 mA/cm^2, allowing each one to operate at its maximum power. The subcells were externally connected in a six terminal series configuration and tested under AM 1.5 global 1-sun illumination as a proof of principle of the InP-based multijunction design [Figure 3(a)]. The spectrum was optically split by using 850 and 1200 nm long-pass filters on top of the InGaAsP middle and InGaAs bottom subcells, respectively, in order to mimic the behavior of the 3-junction device. The tandem activity is demonstrated by the V_{oc}, equal to 1.8 V (modeled max $V_{oc} = 2.1$ V). The J_{sc} (10.3 mA/cm^2) of the externally series-connected solar cell slightly decreased, due to the resistance and possible leakage current within the electrical contacts between the subcells. The spectral response of the independent subcells was measured as a function of wavelength [Figure 3(b)]. All independent single junction solar cells were coated with appropriate anti-reflection coatings to minimize reflection and improve light absorption. All subcells showed maximum EQE around 80%, efficiently absorbing light from a wide range of the spectrum.

As a further step towards the realization of the optimized device, we fabricated an InP-based 3J solar cell[23] and tested it under 1-sun direct illumination [see Figure 4(a)]. For the first test cell structure, features such as the transparent $In_{0.35}Al_{0.65}As$ window layer and back surface field were omitted. Additionally, both the middle InGaAsP and bottom InGaAs subcells thicknesses were reduced to 1 μm from their optimal thicknesses. The monolithically grown 3J device shows similar performance compared to the independently connected subcells. This demonstrates the extremely low resistance of the fabricated tunnel junctions, validating our device modeling assumption for the lattice-matched optimized 3-junction solar cells presented earlier.

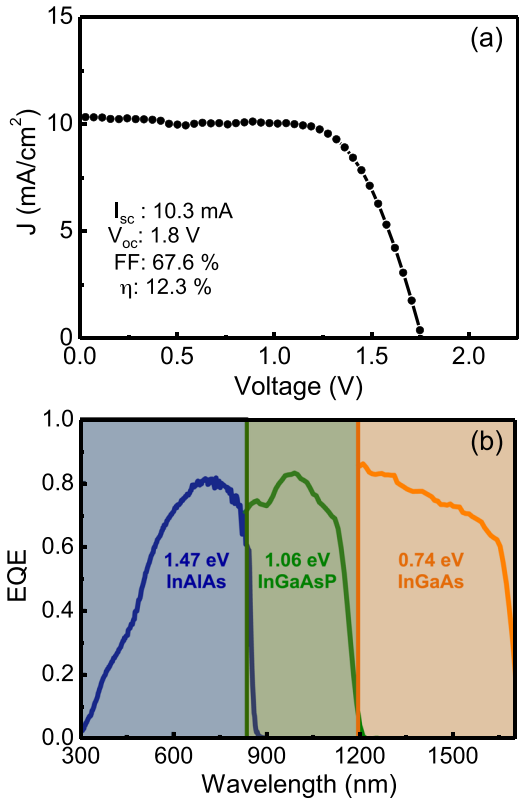

FIG. 3. (a) Light *J-V* curve under 1-sun AM1.5 global illumination for the InAlAs, InGaAsP and InGaAs subcells lattice-matched to InP externally connected in series, in a six terminal configuration. 850 and 1200 nm long pass filters were used on top of the InGaAsP middle and InGaAs bottom subcells, respectively, in order to mimic the behavior of the 3-junction device. (b) External quantum efficiency measurements for each independent subcell.

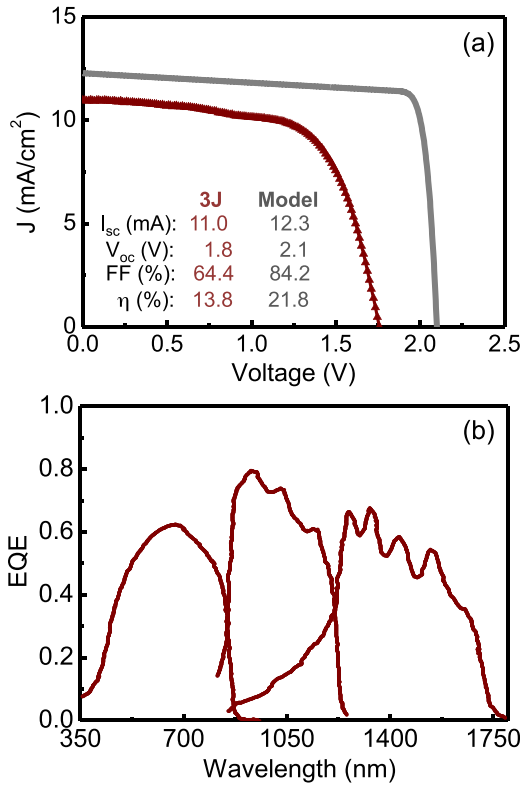

FIG. 4. (a) Light *J-V* curve measured under 1-sun AM1.5 direct illumination for the InP-based 1.47 eV InAlAs/1.06 eV InGaAsP/0.74 eV InGaAs 3-junction device (red triangles), and obtained from 1-dimensional device modeling (grey solid line). (b) External quantum efficiency for the InP-based 3J solar cell.

The device modeling for the InP-based 3J solar cell is also displayed in Figure 4(b). A practical efficiency of 20% (with $V_{oc} \sim 2.0$ V) is expected to be achieved by improving the design in the following aspects: (i) by adding window and back surface field layers to the top InAlAs subcell,[20] which reduces front and back surface recombination velocity, as well as light absorption loss; (ii) by incorporating an anti-reflection coating optimized for this particular band gap combination; and (iii) by thickening the middle and the bottom subcells in order to fully absorb the long wavelength portion of the spectrum and improve the 3J spectral response. Although the efficiency of this InP-based 3J solar cell is far from the theoretical prediction, the results are promising and demonstrate the capability of growing high quality Al-rich epitaxial layers, very low resistance tunnel junctions, and an integrated all lattice-matched multijunction solar cell.

Summarizing, we describe an alternative pathway for a lattice-matched monolithic MJSCs formed by 1.93 eV InAlAs/1.39 eV InGaAsP/0.94 eV InGaAs compound semiconductors. That allows for a better current-match, as shown by detailed balance calculations and device modeling. Theoretically, this design can achieve efficiencies >51% under 100-suns, with $V_{oc} = 3.3$ V, very promising for CPV. As a proof of concept for the suggested 3-junction design, we fabricated an equivalent III-V semiconductor solar cell lattice-matched to InP. Both the series-connected independent subcells and the tandem 3J solar cell presented similar performance, with $V_{oc} = 1.8$ V (for modeled cell $V_{oc} = 2.1$ V). By optimizing the anti-reflection coating and thicknesses of the subcells, one can expect efficiencies around 20% under 1-sun illumination. A maximum EQE of 80% was measured for each subcell. The demonstration of InP-based 3-junction solar cells is an important step towards the development of the multijunction device with optimized band gaps, which is a promising alternative for ultra-high efficiency CPV systems.

The authors acknowledge M. J. Archer, M. D. Kelzenberg, R. R. King, and financial support from the Department of Energy—Solar Energy Technologies Program under Grant No. DE-FG36-08GO18071. MSL acknowledges support under the Cooperative Research Agreement between the University of Maryland and the National Institute of Standards and Technology Center for Nanoscale Science and Technology, award 70NANB10H193, through the University of Maryland.

[1]S. Kurtz and J. Geisz, Opt. Express **18**, A73 (2010).
[2]J. Olson, T. Gessert, and M. Al-Jassim, in *Proceedings of the 18th IEEE Photovoltaic Specialists Conference* (IEEE, New York, 1985), p. 552.
[3]H. Cotal, C. Fetzer, J. Boisvert, G. Kinsey, R. King, P. Hebert, H. Yoon, and N. Karam, Energy Environ. Sci. **2**, 174 (2009).
[4]A. Luque and S. Hegedus, *Handbook of Photovoltaic Science and Engineering* (Wiley, 2011).
[5]A.G. Imenes and D. R. Mills, Sol. Energy Mater. Sol. Cells **84**, 19 (2004).
[6]R. R. King, Nat. Photonics **2**, 284 (2008).
[7]A. Luque, J. Appl. Phys. **110**, 031301 (2011).
[8]J. M. Olson, S. R. Kurtz, A. E. Kibbler, and P. Faine, Appl. Phys. Lett. **56**, 623 (1990).
[9]K. A. Bertness, S. R. Kurtz, D. J. Friedman, A. E. Kibbler, C. Kramer, J. M. Olson, Appl. Phys. Lett. **65**, 989 (1994).
[10]R. R. King, D. C. Law, K. M. Edmondson, C. M. Fetzer, G. S. Kinsey, H. Yoon, R. A. Sherif, and N. H. Karam, Appl. Phys. Lett. **90**, 183516 (2007).
[11]J. F. Geisz, S. Kurtz, M. W. Wanlass, J. S. Ward, A. Duda, D. J. Friedman, J. M. Olson, W. E. McMahon, T. E. Moriarty, and J. T. Kiehl, Appl. Phys. Lett. **91**, 023502 (2007).
[12]R. R. King, A. B. , W. Hong, X.-Q. Liu, D. Bhusari, D. Larrabee, K. M. Edmondson, D. C. Law, C. M. Fetzer, S. Mesropian, and N. H. Karam, in *Proceedings of the 24th European Photovoltaic Solar Energy Conference* (Hamburg, 2009), p. 55.
[13]R. R. King, D. Bushari, D. Larrabee, X.-Q. Liu, E. Rehder, K. Edmondson, H. Cotal, R. K. Jones, J. H. Ermer, C. M. Fetzer, D. C. Law, and N. H. Karam, Prog. Photovoltaics **20**, 801 (2012).
[14]M. Wiemer, V. Sabnis, and H. Yuen, *Proceedings of the SPIE Optics + Photonics − Solar Energy + Technology* (San Diego, 2011).
[15]J. M. Zahler, K. Tanabe, C. Ladous, T. Pinnington, F. D. Newman, and H. A. Atwater, Appl. Phys. Lett. **91**, 012108 (2007).
[16]N. Szabo, B. E. Sagol, U. Seidel, K. Schwarzburg, and T. Hannappel, Phys. Status Solidi (RRL) **2**, 254 (2008).
[17]M. W. Wanlass, T. I. Coutts, J. S. Ward, K. A. Emery, T. A. Gessert, and C. R. Osterwald, in *Proceedings of the 22nd IEEE Photovoltaic Specialists Conference* (IEEE, 1991), p. 38.
[18]Here, the optimization refers to the best band gap combination corresponding to semiconductor compounds with lattice spacing between GaAs and InP, therefore the design is termed "optimized."
[19]R. Stangl, M. Kriegel, and M. Schmidt, in *Proceedings of the 4th World Conference on Photovoltaic Energy Conversion* (IEEE, New York, 2006), p. 1350.
[20]M. S. Leite, R. L. Woo, W. D. Hong, D. C. Law, and H. A. Atwater, Appl. Phys. Lett. **98**, 093502 (2011).
[21]M. S. Leite, E. C. Warmann, G. M. Kimball, S. P. Burgos, D. M. Callahan, and H. A. Atwater, Adv. Mater. **23**, 3801 (2011).
[22]The crystal quality of the subcells was analyzed by high resolution x-ray diffraction measurements using a conventional Cu-K x-ray source. The x-ray beam size was 4×25 mm^2, giving an accurate and representative estimative of the crystal diffraction condition, and therefore its lattice constant. (004) symmetric ω-2θ scans were performed to confirm that the material grown was lattice-matched to the InP substrate.
[23]R. L. Woo, W. D. Hong, S. Mesropian, M. S. Leite, H. A. Atwater, and D. C. Law, in *37th Photovoltaic Specialists Conference* (IEEE, Seattle, 2011).